Clay Dispersed Styrene-co-Glycidyl Methacrylate Impregnated Kumpang Wood Polymer Nanocomposites: Impact on Mechanical and Morphological Properties

Md. Tipu Sultan,[a,*] Md. Rezaur Rahman,[a] Sinin Hamdan,[b] Josephine Chang Hui Lai,[a] and Zainal Abidin Talib [c]

Physical, mechanical, and morphological properties of a clay dispersed styrene-co-glycidal methacrylate (ST-co-GMA) impregnated wood polymer nanocomposite (WPNC) were evaluated. The WPNC was characterized by Fourier transform infrared spectroscopy (FTIR), scanning electron microscopy (SEM), 3-point bending, free-vibration testing, and X-ray diffraction (XRD) measurements. The FT-IR results showed that the absorbance at 1730 cm^{-1} was increased for ST-co-GMA-clay-WPNC compared with other nanocomposites and the raw material. The XRD results revealed that crystallinity index and d-spacing were increased compared to raw wood. The SEM results showed that ST-co-GMA-clay-WPNC had a smoother surface than other nanocomposites and raw wood. The modulus of elasticity (MOE), modulus of rupture (MOR), and dynamic Young's moduli (Ed) of WPNCs were considerably increased compared to wood polymer composites (WPCs) and raw wood. The raw wood exhibited a higher water uptake (WU) than WPNCs and WPCs.

Keywords: ST-co-GMA; Nanoclay; Mechanical properties; Morphological properties

*Contact information: a: Department of Chemical Engineering and Energy Sustainability, Faculty of Engineering, Universiti Malaysia Sarawak, 94300 Kota Samarahan, Sarawak, Malaysia; b: Department of Mechanical Engineering, Faculty of Engineering, Universiti Malaysia Sarawak, 94300 Kota Samarahan, Sarawak, Malaysia; c: Department of Physics, Faculty of Science, Universiti Putra Malaysia, 43400 UPM Serdang, Selangor, Malaysia; *Correspondent author: tipuchem75@gmail.com*

INTRODUCTION

Wood has a remarkable value and importance in the world's economy because of its mechanical, renewable, sustainable, and eco-friendly characteristics (Zabel and Morrell 1992). Wood has attracted attention by material researchers for replacing synthetic plastic materials, which are not renewable or eco-friendly (Mohanty *et al.* 2002; Bledzkiet *et al.* 2007; Rahman *et al.* 2015). Wood is also used as a material for musical instruments because of its wide-ranging colors and acoustic properties (Hamdan *et al.* 2010). The natural frequency of a wood beam can determine the cracks present in the wood, which affects the dynamic behavior of wood (Kam and Lee 1992). Wood is a natural composite that is composed of cellulose, hemicellulose, and lignin. These constituents can be regarded as a series of tubular fibers or cells cemented together. Cellulose is responsible for wood strength because of its linear orientation and high degree of polymerization. Hemicelluloses and lignin are also closely associated with cellulose to increase the packing density of the cell wall. Hemicelluloses act as a coupling agent to bind non-crystalline hydrophilic cellulose and amorphous hydrophobic lignin. Cellulose, hemicellulose, and lignin are responsible for the mechanical properties of wood. The macromolecule of cellulose is formed by covalent bonding, which is resistant to tensile stress. The hydrogen

bonds within the cellulose provide rigidity by transferring stress. The mechanical properties of wood also depend on temperature, pressure, humidity, pH, chemical adsorption from the environment, UV radiation, fire, and biological degradation. At high humidity, wood is dimensionally unstable and susceptible to termite attack because of its hydrophilic and capillarity properties (Rowell 2006). In low-humidity environments, wood desorbs water and undergoes shrinkage. Hygroscopic and dimensionally unstable properties restrict the use of wood. In outdoor applications, wood suffers from the photodegradation process as well (Mattos *et al.* 2014). Wood also discolors when used indoor as a result of the oxidation of lignin, albeit with a lower rate (Feist and Hon 1984).

When wood plastic composites (WPCs) first entered the market, the wood particles were presumed to be completely encapsulated in the plastic, thereby protecting them from both moisture and microorganism attack (Morrell *et al.* 2006). However, this impermeable conception is not completely true. For fast-growing wood, the mechanical properties, color stability, and durability are not satisfactory because of its low density and water uptake. To overcome these drawbacks, modified wood such as WPCs and wood composites are used as wood materials instead of conventional wood material (Chang and Chang 2001a,b; Cao *et al.* 2011, Hamdan *et al*. 2012). To decrease the hydrophilicity and fungal attack of wood materials, various chemical treatments have been introduced, such as acetylation, benzylation, and silane or maleic anhydride grafting. In all these cases, the chemicals react with the –OH group of the cell lumen and cell cavity of wood (Xie *et al.* 2011). The use of hydrophobic thermoplastic fillers, without any reaction with wood, also improves the mechanical performance of wood by filling the cell cavities of wood. Heat treatment, hydrothermal treatment, oil heat treatment, hot pressing treatment, and *in situ* polymerization can also eliminate or decrease the disadvantages of wood (Li *et al.* 2013; Islam *et al.* 2014).

Polymer nanocomposites are polymers (thermoplastics, thermosets, or elastomers) that have been reinforced with small quantities (usually less than 5% by weight) of very high-aspect ratio ($l/t > 300$) fillers in its matrix (Hegde 2009). In wood polymers, the nanocomposite nanofiller used will form an adhesive bond with wood. The adhesive bonds in wood composites hold elements of the composite together by their bond strength and transfer stress across the bond line between the bonded wood elements. For wood properties such as modulus or thermal and moisture expansion coefficients, the bond stiffness is more important than bond strength (Le *et al.* 2014). In wood polymer nanocomposites, the chemically modified wood is also photostable (Prakash and Mahadevan 2008; Farahani and Taghizadeh 2010; Jebrane *et al.* 2011).

Eucalyptus grandis does not exhibit good mechanical performance because of its low permeability for impregnation of styrene and methyl methacrylate monomers (Stolf and Lahr 2004). However, wood flour coated with the hydrophilic-hydrophobic block-copolymer based on styrene and acrylic acid shows a significant improvement in the ultimate tensile properties of the composite (Kosonen *et al.* 2000). The compatibility between wood and nonpolar polymers such as styrene, ethylene, and vinyl acetate can be improved using glycidyl methacrylate (GMA) as a compatibilizer (Devi and Maji 2007; Dikobe and Luyt 2007). The plasticized wood composite increases the mechanical properties and decay resistance (Rahman *et al.* 2010) of wood. Nanoclay, by binding to hydroxyl groups of wood components, improves the interaction between wood and thermoplastic polymer (Agubra *et al.* 2013).

Montmorillonite (MMT) has two outer tetrahedral layers which contain Si and O atoms. These layers organize themself to form stalks by Van der Waals force of attraction

between them. The attraction force between layers is relatively weak, so polymer molecules can be intercalated between them. The intercalated polymer molecules are dispersed into wood cell wall to produce wood polymer composites (Carroll 1970; Bhattacharya and Aadhar 2014). With respect to a wood and copolymer macromolecular composite system, montmorillonite intercalated polymer molecules can be dispersed different ways into the wood. The particles of MMT intercalated polymer molecules can be homogeneously dispersed into the macropores of wood. MMT itself can directly enter into the wood cell wall and form adhesive bonds at the molecular level (Zhao *et al.* 2006). The MMT intercalated polymer strengthen the mechanical properties of wood and make the wood resistant to water uptake and microorganisms (Baysal *et al.* 2007; Xu *et al.* 2013). Polymer–clay nanocomposites have emerged as a fascinating field of research because of their multiple advantages, which include an improvement in mechanical, dimensional, and thermal properties.

The present study investigates the physico-mechanical and morphological properties of clay dispersed styrene-co-glycidyl methacrylate (St-co-GMA-clay) impregnated wood polymer nanocomposites (WPNCs). The morphological properties are also reported in this study.

EXPERIMENTAL

Materials

Five wood specimens were chosen for this study. These wood specimens were impregnated by styrene (ST) (A. S. Joshi and Company, Goregaon West, Mumbai), glycidyl methacrylate (GMA) (Aldrich, USA), and nanoclay (Nanomer^{R}1.28E) that had been modified with 25 to 30 wt.% trimethyl stearyl ammonium (Aldrich, USA). Benzoyl peroxide (Merck Schuchardt OHG, Germany) was used in the system as a catalyst to increase the reaction rate by a free radical mechanism.

Specimen Preparation

A Kumpang tree was cut into three bolts 1.2 m long. Each bolt was quarter-sawn to produce planks 4 cm thick. These planks were subsequently conditioned by air drying in a room with a relative humidity of 60% and ambient temperature of approximately 25 ^{o}C for one month prior to testing. The planks were ripped and machined to 340 mm (L) x 20 mm (T) x10 mm (R) for three-point bending and free-free vibration tests.

Preparation of Wood Polymer Nanocomposites (WPNCs)

Oven-dried specimens were impregnated with 500 mL of styrene (St), a mixture of 500 mL of styrene with 10 gm MMT, a mixture of 500 mL of styrene with glycidyl methacrylate (1:1 ratio), and 10 gm MMT. The four different solution mixtures were used to impregnate the wood specimens. The wood specimens were then separately placed in an impregnation vacuum chamber of 75 mm (Hg) for 30 min. In each system, approximately 10 g of benzoyl peroxide was added as the initiator. These wood composites were then removed from the chamber, and the excess chemicals were wiped off. Specimens wrapped with aluminum foil were placed in an oven for 24 h at 105 ^{o}C for polymerization to take place. Weight percentage gain (WPG) was calculated from the following equation,

$$\text{WPG\%} = \frac{W_f - W_i}{W_i} \times 100 \quad (1)$$

where W_f and W_i are the oven-dried weight of the WPC and raw wood, respectively.

Table 1. Composition of the Chemicals for Raw Wood Impregnation

SL	Specimen	ST	GMA	Clay
1	Raw wood (RW)			
2	RW	500 mL		
3	RW	500 mL	500 mL	
4	RW	500 mL		10 gm
5	RW	500 mL	500 mL	10 gm

Determination of Water Uptake

Percentage water uptake (WU) after two weeks at 30 °C was calculated according to Eq. 2,

$$WU\% = \frac{W_2 - W_1}{W_1} \times 100 \quad (2)$$

where W_2 is the weight of a wood sample, treated and untreated, after two weeks of water immersion and W_1 is the weight of an oven-dried sample.

Characterization

Fourier transform infrared spectroscopy (FTIR)

The infrared spectra of all specimens were recorded on a Shimadzu FT-IR 81001 Spectrophotometer (Kyoto, Japan). The transmittance range of the scan used was 4000 to 600 cm^{-1}.

Modulus of rupture (MOR), Modulus of elasticity (MOE), and dynamic Young's modulus (E_d) measurements

Three-point bending tests were conducted according to Shimadzu MSC-5/500 universal testing machine (Kyoto, Japan) operating at a crosshead speed of 5 mm/min.

MOR and MOE were calculated as follows,

$$MOR = \frac{1.5LW}{bd^2} \quad (3)$$

$$MOE = \frac{L^3 m}{4bd^3} \quad (4)$$

where W is the ultimate failure load, L is the span between centers of support, b is the mean width (tangential direction) of the sample, d is the mean thickness (radial direction) of the sample, and m is the slope of the tangent to the initial line of the force displacement curve.

Determination of E_d for all specimens was carried out using a free-free flexural vibration testing system. The E_d was calculated from the resonant frequency using the following equation,

$$E_d = \frac{4\Pi^2 f^2 l^4 A\rho}{I m_n^4} \quad (5)$$

where $I = bd^3 / 12$, d is the beam depth, b is the beam width, l is the beam length, f is the natural frequency of the specimen, ρ is the density, A is the cross-sectional area, and $n = 1$ is the first mode of vibration, where $m_1 = 4.730$.

X-ray Diffraction (XRD) analysis

XRD analysis for raw wood and wood polymer nanocomposites were performed with a Rigaku diffractometer (CuK$_\alpha$ radiation, λ= 0.154 nm) running at 40 kV and 30 mA. An experimental procedure for the determination of degree of crystallinity is acceptable to these materials in as much as X-ray scattering curves are resolvable into crystalline and amorphous scattering regions. The crystallinity index (CI$_{XRD}$) was calculated using the following height ratio,

$$\text{CI}_{\text{XRD}}\ (\%) = \frac{I_{002} - I_{am}}{I_{002}} \quad (6)$$

where I_{002} is the intensity of the 002 crystalline peak at 22° and I_{am} is the height of the minimum (I_{am}) between the 002 and the 004 peaks, as shown in Fig. 5. The d-spacing of 002 lattice planes of the sample was calculated from the Bragg equation,

$$d = \frac{n\lambda}{2\,sin\theta} \quad (7)$$

where λ is the X-ray wavelength (0.154 nm).

Scanning electron microscopy (SEM)

The fractured surface was used to examined see the interfacial bonding between wood cell and polymer with filler by Hitachi (TM 3030) scanning electron microscope (SEM) supplied by JEOL (Tokyo, Japan). The SEM specimens were sputter-coated with gold prior to observation. The micrographs were acquired at a magnification of 1.5k.

RESULTS AND DISCUSSION

FTIR

The FTIR spectra of various samples are presented in Fig. 1. The peak from 4000 to 3000 cm^{-1} corresponds to stretching vibration of H-bonds in -OH groups, and C-H stretching in methyl and methylene groups range from 3000 to 2800 cm^{-1} (Hamdan *et al.* 2011). The peak intensity near 1505 cm^{-1} (for aromatic double bonds) was higher for ST impregnated wood than for raw wood. This was due to the increase in the concentration of aromatic groups in the ST–WPC specimens. The IR spectra of ST–WPC samples exhibited a peak intensity above 3000 cm^{-1} for the -OH group that was lower than that of raw wood because of the removal of free-bound water from the wood lumen by ST. The peak intensity of the –OH group for ST-co-GMA impregnated wood was lower than that of ST impregnated wood because of the covalent bond formed between the –OH of wood and the glycidyl group of GMA. This can be attributed to the fact that ST-co-GMA performs better as a filler than ST alone. In the case of the ST-co-GMA-clay-WPNC composite, for wavenumbers above 3000 cm^{-1}, the peak intensity did not decrease compared with raw wood. The peak intensity above 3000 cm^{-1} increases with the clay ST-co-GMA polymer system, which removed fewer –OH groups from cellulose, hemicellulose, and water in the wood lumen. The −OH group of montmorillonite in the composite indicated absorption peak near 840 cm^{-1} for the Mg-Al-OH linkage (Sposito 1983). The absorption peak near 905 cm^{-1} was more intense in the ST-co-GMA-clay-WPNC system than the other ones. The peak intensity near 1730 cm^{-1} increased because of the increase in carbonyl group content in the composite compared with the raw wood. Because of the addition of

montmorillonite in the ST-co-GMA-clay-WPNC system, the carbonyl peak intensity was higher than that in the ST-co-GMA system. This occurs because of the copolymerization between ST and GMA for the exfoliation of montmorillonite in the wood.

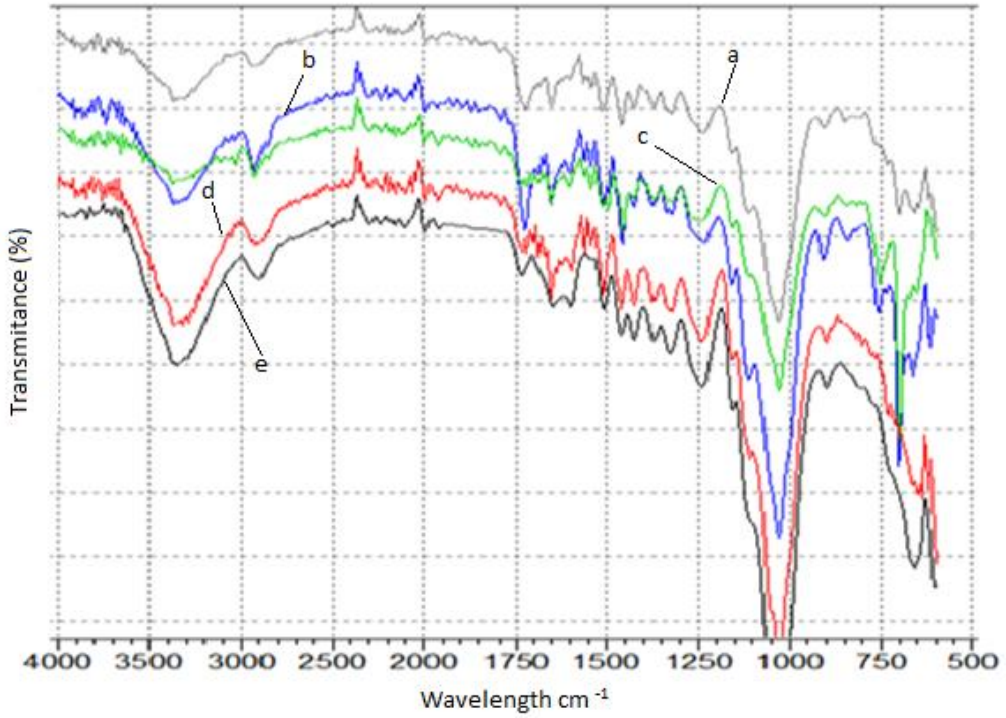

Fig. 1. FTIR spectra of a) ST-co-GMA-WPC, b) ST-co-GMA-clay-WPNC, c) ST-Clay-WPNC, d) ST-WPC, and e) RW

The reaction scheme is shown in Fig. 2.

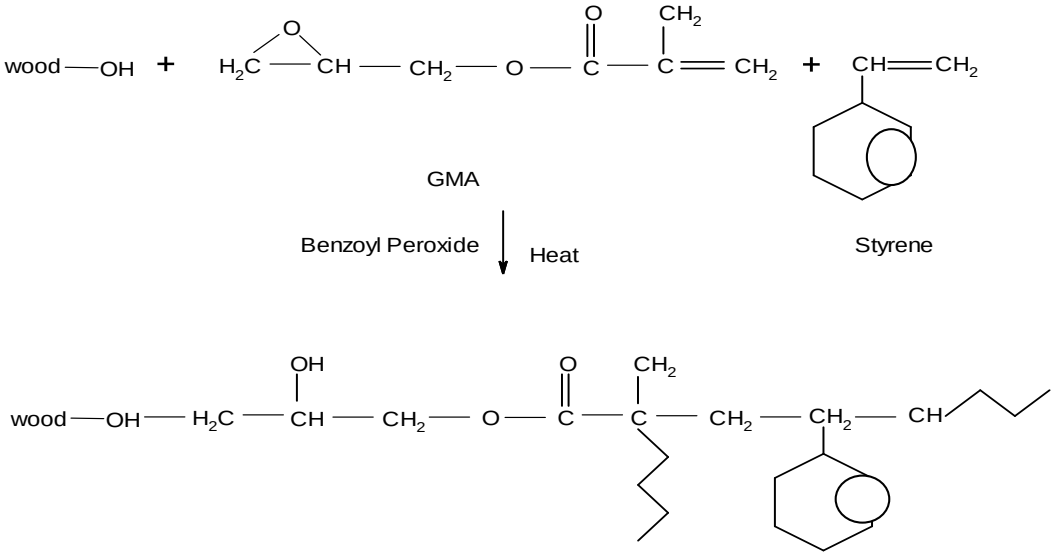

Fig. 2. Schematic reaction diagrams

MOR, MOE, and E_d

The MOE, MOR, and E_d analyses of the raw wood and four different WPC materials are given in Fig. 3

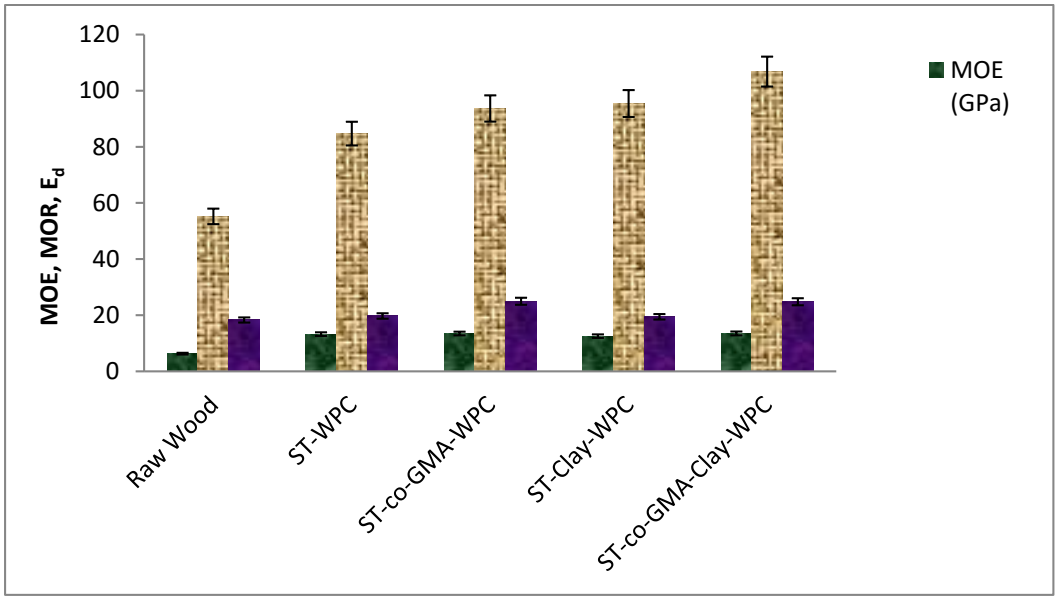

Fig. 3. MOE, MOR and E_d of a) RW, b) ST-WPC, c) ST-co-GMA-WPC, d) ST-Clay-WPNC, and e) ST-co-GMA-Clay-WPNC

As shown in Fig. 3, the composites exhibited higher MOE and MOR than the raw wood. This was attributed to the presence of a filler that exerts Van der Waals force and forms covalent bonds with the wood cell wall. In the ST–WPC, there exists only Van der Waals force between wood and ST, so it has lower MOE and MOR compared with ST-Clay-WPNC and ST-GMA-Clay-WPNC specimens. The clay particles have high surface area and possess charges that form dipole bonds as well as Van der Waals forces with the wood cell wall. The MOE and MOR values were the highest for ST-co-GMA-clay-WPNC among these five composites. The epoxy group of GMA formed a covalent bond with the –OH group of wood, and the vinyl group reacted with styrene by a free radical mechanism. Thus, the polymers and the wood cell walls achieved a sufficiently strong chemical bonding strength (Rashmi *et al.* 2008; Rahman *et al.* 2015). Also, MMT intercalates in the ST-co-GMA and a maximum number of MMT exfoliates in the St-co-GMA that has filled the wood cavities and thus increases the MOE and MOR of wood. On the other hand, in the ST-Clay impregnated WPNCs showed intercalation rather than the exfoliation. Therefore, the MOE and MOR of ST-co-GMA-clay impregnated WPNCs were higher than that of ST-Clay impregnated WPNC.

Among the composites, the highest E_d was observed for the ST-co-GMA-clay-WPNC, followed by ST-co-GMA-WPC, ST-WPC, and ST-Clay-WPNC. This is due to an increase in the density and shear force in the wood composite (Rahman *et al.* 2010). In the presence of shear force, the free energy increases and the molecules continuously oscillate from equilibrium (Toh 1979). The shear force is considered to vary sinusoidally with time. The styrene monomer cannot directly react with wood cell wall components, whereas ST-co-GMA reacts with cell wall components to produce the covalent bond. The large clay particles enter the wood, which increase the Van der Waals forces in the composite to increase shear stress.

Weight Percentage Gain (WPG) and Water Uptake (WU)

Both WPG and WU values are shown in Fig. 4. It is clear that ST-co-GMA-Clay-WPNC showed higher WPG% compared with the other composites. This is due to the presence of epoxy groups, which form covalent bonds with the –OH group of wood as well as deposition of polymers which is facilitated by the crosslinking reaction. The vinyl group present reacts with styrene by a free radical mechanism which exfoliates MMT in the St-co-GMA monomer system that filled the wood cavities. ST-co-GMA-Clay-WPNC had higher exfoliation, whereas ST-Clay-WPNC showed intercalation.

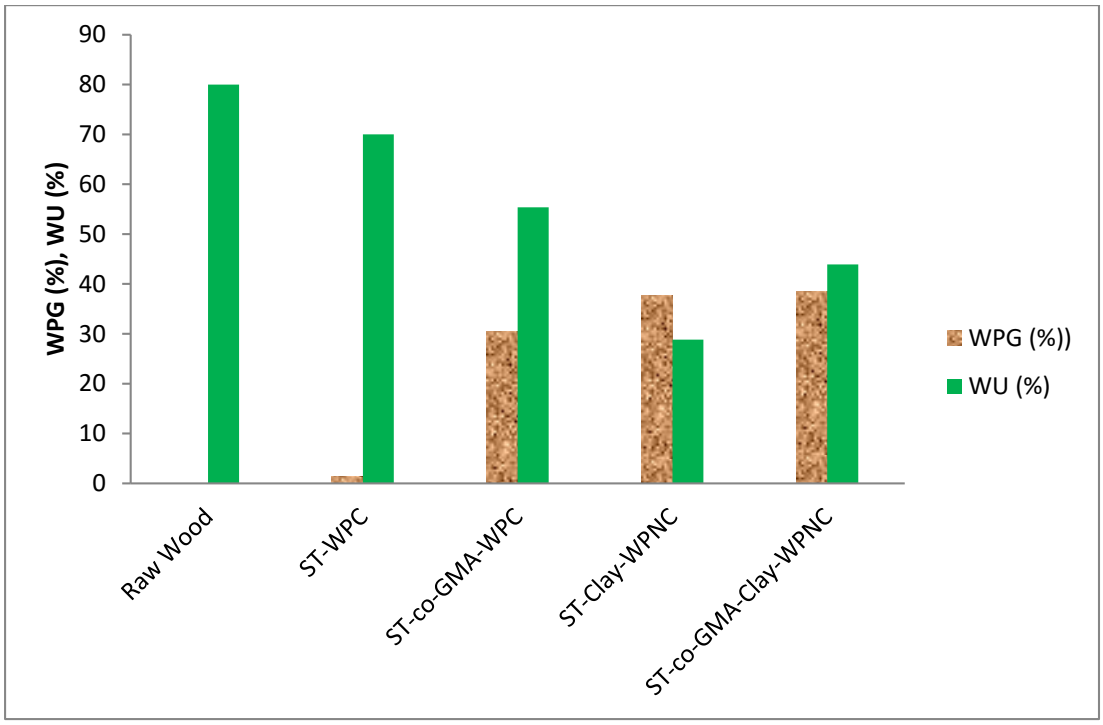

Fig. 4. WPG (%), and WU (%) of a) RW, b) ST-WPC, c) ST-co-GMA-WPC d) ST-Clay-WPNC, and e) ST-co-GMA-Clay-WPNC

The water absorption of various samples is illustrated in Fig. 4. The raw wood sample exhibited a higher percentage of water absorption compared with the modified WPCs. This was expected because ST, ST-clay, ST-co-GMA, and ST-co-GMA-Clay had reduced pore size on the surface of the wood (Rahman *et al*. 2010). The void area on the wood surface facilitates water penetration into the wood cell wall with hydrophilic hydroxyl groups. Styrene-GMA-treated samples absorbed less water than styrene-treated samples because more void areas are present in ST-WPC compared with ST-co-GMA-WPC, which is also reflected in the SEM analysis. Similar results have been reported for rubber wood samples (Devi and Maji 2007). It is also apparent that ST-Clay-WPNC had the lowest (28.84%) water absorption of all the samples. This is due to the surface modified MMT with alkyl group.

X-ray Diffraction (XRD) Analysis

X-ray diffractograms of raw wood, WPCs, and WPNCs are shown in Fig. 5. The diffraction pattern of WPCs and WPNCs exhibited crystalline content as well as a broad amorphous region, whereas raw wood showed just an amorphous region. The values of 2θ

were around 22.4° for raw wood, WPCs, and WPNCs, which are assigned to the [002] crystalline plane. However, the values of 2θ = 36 ° shown as [040] plane and crystallinity index CI_{XRD} was determined at [002] plan which is shown in Table 2. (Masahisa *et al.* 2004; Chen *et al*. 2016). Among them the CI_{XRD} was highest for ST-WPC because styrene does not react with the OH group; instead, it restricts the movement of amorphous chains (Victor *et al.* 2013). The CI_{XRD} of ST-Clay-WPNC was higher than ST-co-GMA-clay-WPNC due to removal of –OH groups from cellulose molecules by GMA. The values of 2θ for WPCs and WPNCs were decreased compared to raw wood, whereas the d-spacing of [002] plane increased. The increment of d-spacing indicated that the wood sample was successfully impregnated by polymer (Tingje *et al*. 2016).

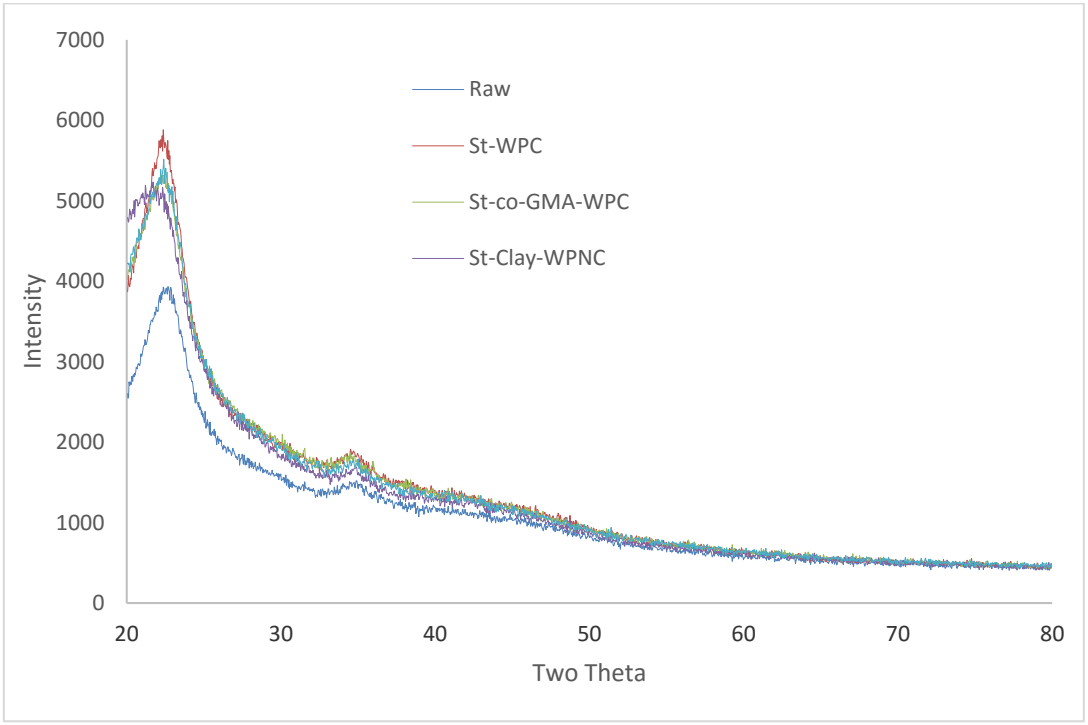

.

Fig. 5. X-ray diffraction (XRD) diffractograms of a) RW, b) ST-co-GMA-WPC, c) ST-co-GMA-Clay-WPNC d) ST-Clay-WPNC, and e) ST-WPC

Table 2. Crystallinity Index CI_{XRD} and D-spacing as Obtained by XRD Analysis

Sample	CI_{XRD}(%)	D-Spacing (002)nm	2θ (002)
Raw	66.59	0.3913	22.6967
ST-WPC	72.5	0.3970	22.3667
ST-co-GMA-WPC	69.34	0.3923	22.6367
ST-Clay-WPNC	71.89	0.4089	21.7067
ST-co-GMA-clay-WPNC	71.4	0.3964	22.3997

Although some –OH groups were reduced by GMA, the CI_{XRD} of all composites increased compared to the raw sample. This is due to the reduction of amorphous movement. Among the composites, there was no additional peak with respect to raw wood.

Scanning Electron Microscopy (SEM)

The scanning electron micrographs are shown in Figs. 6(a), (b), (c), and (d). It was observed that the lumen and tracheids of wood had been filled by the solid polymers by *in situ* polymerization.

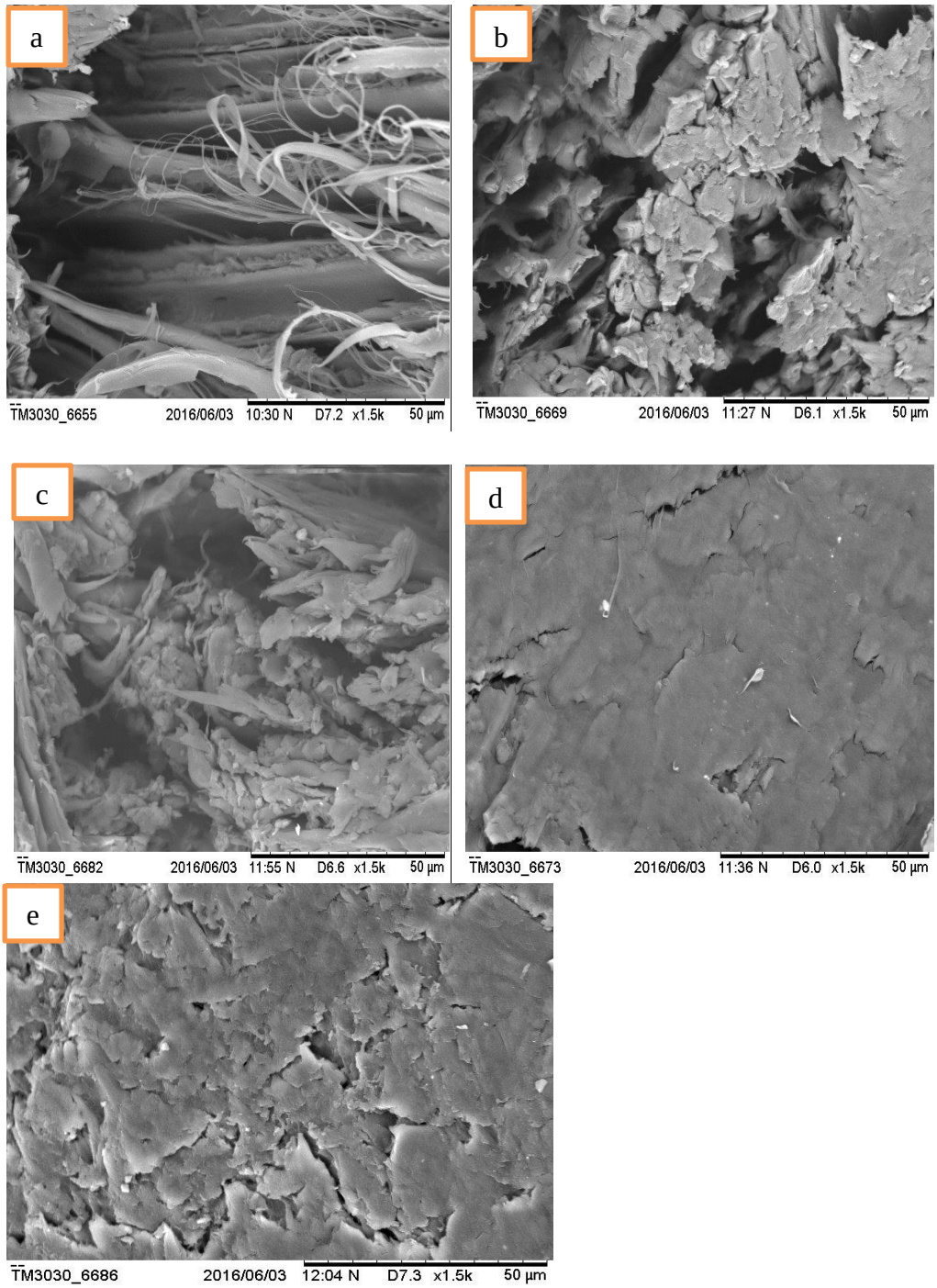

Fig. 6. SEM micrographs of (a) RW; (b) ST-WPC; (c) ST-co-GMA-WPC; (d) ST-Clay-WPNC; and (e) ST-co-GMA-Clay-WPNC

From Fig. 6(d) and (e), the wood surfaces were smoother than the RW, ST-WPC, and ST-co-GMA. This is due to the intercalation of MMT in the composites system that filled the void spaces of wood; this is reflected in the XRD analysis. However, Fig. 6(a) showed that there was unfilled cell wall and pore volume, whereas ST-WPC partially filled cell wall and pore volume (Fig. 6(b)). On the other hand, ST-co-GMA-WPC moderately filled the cell walls and pores, as shown in Fig. 6(c). Styrene itself and ST-co-GMA could not fill the maximum number void spaces of raw wood compared to ST-Clay and ST-co-GMA-Clay. The poor interaction between the polymer and wood implied a more brittle composite (Li *et al.* 2011). Therefore, it was concluded that there were strong interactions among the polymers, MMT, and wood cell walls, as shown in Fig. 6 (d) and (e).

CONCLUSIONS

1. Kumpang wood was successfully impregnated by clay dispersed styrene-co-glycidyl methacrylate (St-co-GMA-clay) which was demonstrated by FT-IR and XRD analysis.
2. WPNCs had the highest MOE, MOR, and E_d values, followed by WPCs and RW.
3. ST-co-GMA-Clay-WPNC specimens showed the highest WPG, followed by ST-clay, ST-co-GMA, and ST.
4. ST-clay-WPCs had lower water uptake than ST-co-GMA-Clay-WPNC, ST-co GMA-WPCs, ST-WPCs, and raw wood.
5. The SEM morphology showed that ST-co-GMA-Clay-WPNC had a smoother surface than ST-Clay-WPCs, ST-co-GMA-WPCs, ST-WPCs, and raw wood.

ACKNOWLEDGMENTS

This work was financially supported by University of Malaysia Sarawak under the grant number FRGS/SG02(01)/1085/2013(31).

REFERENCES CITED

Agubra, V. A., Owuor, P. S., and Hosur, M. V. (2013). "Influence of nanoclay dispersion methods on the mechanical behavior of E-glass/epoxy nanocomposites," *Nanomaterials* 3(3), 550-563; doi:10.3390/nano3030550).

Baysal, E., Yalinkilic, M. K., Altinok, M., Sonmez, A., Peker, H., and Colak, M. (2007). "Some physical, biological, mechanical, and fire properties of wood polymer composite (WPC) pretreated with boric acid and borax mixture," *Construction and Building Materials* 21(9), 1879-1885. DOI: 10.1016/j.conbuildmat.2006.05.026

Bhattacharya, S. S., and Aadhar, M. (2014). "Studies on preparation and analysis of organoclay nano particles," *Research Journal of Engineering Sciences* 3(3), 10-16.

Bledzki, A. K., Mamun A. A., and Faruk, O. (2007). "Abaca fibre reinforced PP composites: Comparison with jute and flax fibre composites considering fibre contents," *eXPRESS Polymer Letters* 1(11), 755-762. DOI: 10.3144/expresspolymlett.2007.104

Cao, Y., Lu, J., Huang, R., Zhao, Y., and Wu, Y. (2011). "Evaluation of decay resistance for steam-heat-treated wood," *BioResources* 6(4), 4696-4704. DOI: 10.15376/biores.6.4.4696-4704

Carroll, D. (1970). *Clay Minerals: A Guide to Their X-ray Identification*, Special Paper 126, The Geological Society of America, Boulder, CO.

Chang, H. T., and Chang, S. T. (2001a). "Inhibition of the photodiscoloration of wood by butyrylation," *Holzforschung* 55(3), 255-259. DOI: 10.1515/HF.2001.042

Chang, S. T., and Chang, H. T. (2001b). "Comparisons of the photostability of esterified wood," *Polymer Degradation and Stability* 71(2), 261-266. DOI: 10.1016/S0141-3910(00)00171-3

Chen, T. J., Wu, Z. Z., Xie, Y. Q., and Wang, X. D. (2016). "Effect of Si–Al molar ratio on microstructure and mechanical properties of ultra-low density fiberboard," *European Journal of Wood and Wood Products* 74(2), 151-160. DOI 10.1007/s00107-015-0986-x

Devi, R. R., and Maji, K. T. (2007). "Effect of glycidyl methacrylate on the physical properties of wood–polymer composites," *Polymer Composites* 28(1), 1-5. DOI: 10.1002/pc.20265

Dikobe, D. G., and Luyt, A. S. (2007). "Effect of poly (ethylene-co-glycidyl methacrylate) compatibilizer content on the morphology and physical properties of ethylene vinyl acetate," *Wood Fiber Composites* 104(5), 3206-3213. DOI: 10.1002/app.26080

Farahani, M. R. M., and Taghizadeh, F. (2010). "Roughness of esterified eastern cottonwood," *BioResources* 5(4), 2232-2238. DOI: 10.15376/biores.5.4.2232-2238

Feist, W. C., and Hon, D. N. S. (1984). "Chemistry of weathering and protection," in: *The Chemistry of Solid Wood*, R. Rowell (ed.), American Chemical Society, Washington, DC, pp. 401-451. DOI: 10.1021/ba-1984-0207.ch011

Hamdan, S., Rahman, M. R., Ahmed, A. S., Islam, M. S., Talib, Z. A., Abdullah, W. F. W., and Mat, M. S. C. (2011). "Thermogravimetric analysis and dynamic young's modulus measurement of N, N- dimethylacetamide-impregnated wood polymer composites," *Journal of Vinyl and Additive Technology* 17(3), 177-183. DOI: 10.1002/vnl.20275

Hamdan, S., Rahman, M. R., Ahmed, A. S., Islam, M. S., and Talib, Z. A. (2010). "Dynamic young's modulus measurement of treated and post-treated tropical wood polymer composites," *BioResources* 5(1), 324-342. DOI: 10.15376/biores.5.1.324-342

Hamdan, S., Rahman, R. M., Ahmed, A., Hasan, M., and Islam, M. S. (2012). "Effect of coupling reactions on the mechanical and biological properties of tropical," *International Biodeterioration and Biodegradation* 72, 108-113. DOI: 10.1016/j.ibiod.2012.05.019

Hegde, R. R. (2009). *Structure and Properties of Nanoclay Reinforced Polymer Films, Fibers and Nonwovens*, Ph.D. dissertation, University of Tennessee, Knoxville, TN.

Islam, M. S., Hamdan, S., Hassan, A., Sobuz, H., and Talib, Z. A. (2014). "The chemical modification of tropical wood polymer composites," *Journal of Composite Materials* 48(7), 783-789. DOI: 10.1177/0021998313477894

Jebrane, M., Pichavant, F., and Sebe, G. (2011). "A comparative study on the acetylation of wood by reaction with vinyl acetate and acetic anhydride," *Carbohydrate Polymers* 83(2), 339-345. DOI: 10.1016/j.carbpol.2010.07.035

Kam, T. Y., and Lee, T. Y. (1992). "Detection of cracks in structures using modal test data," *Journal of Engineering Fracture Mechanics* 42(2), 381-387. DOI: 10.1016/0013-7944(92)90227-6

Kosonen, M. L., Wang, B., Caneba, G. T., Gardner, D. J. and Rials, T. G. (2000) "Polystyrene/wood composites and hydrophobic wood coatings from water-based hydrophilic-hydrophobic block," *Clean Products and Process,* Springer-Verlag, 2(2000), 117-123.

Le, E. A., and Nairn, J. A. (2014). "Measuring interfacial stiffness of adhesively-bonded wood," *Wood Science and Technology* 48(6), 1109-1121. DOI: 10.1007/s00226-014-0661-0

Li, Y. F., Liu, Y. X., Wang, X. M., Wu, Q. L., Yu, H. P., and Li, J. (2011). "Wood–polymer composites prepared by the *in situ* polymerization of monomers within wood," *Journal of Applied Polymer Science* 119(6), 3207-3216. DOI: 10.1002/app.32837

Li, Y., Liu, Z., Dong, X., Fu, Y., and Liu, Y. (2013). "Comparison of decay resistance of wood and wood-polymer composite prepared by in situ polymerization of monomers," *International Biodeterioration and Biodegradation* 84, 401-406. DOI: 10.1016/j.ibiod.2012.03.013

Masahisa, W., Laurent, H., and Junji, S. (2004). "Polymorphism of cellulose I family: Reinvestigation of cellulose IVI," *Biomacromolecules* 5(4), 1385-1391. DOI: 10.1021/bm0345357.

Mattos, B. D., de Cademartori, P. H. G., Lourencon, T. V., and Gatto, D. A. (2014). "Colour changes of Brazilian eucalypts wood by natural weathering," *International Wood Products Journal* 5(1), 33-38. DOI: 10.1179/2042645313Y.0000000035

Mohanty, A. K., Misra, M., and Drzal, L. T. (2002). "Sustainable bio-composite from renewable resources: Opportunity and challenges in the green materials world," *Polymer and the Environment* 10(1/2), 19-26. DOI: 10.1023/A:1021013921916

Morrell, J. J., Stark, N. M., Pendleton, D. E., and McDonald, A. G. (2006). "Durability of wood-plastic composites," *Wood Design Focus* 16(3), 7- 10

Prakash, G. K., and Mahadevan, K. M. (2008). "Enhancing the properties of wood through chemical modification with palmitoyl chloride," *Applied Surface Science* 254(6), 1751-1756. DOI: 10.1016/j.apsusc.2007.07.137

Rahman, M. R., Hamdan, S., Ahmed, A. S., and Islam, M. S. (2010). "Mechanical and biological performance of sodium metaperiodate-impregnated plasticized wood (PW*)," BioResources* 5(2), 1022-1035. DOI: 10.15376/biores.5.2.1022-1035

Rahman, M. R., Lai, J. C. H., Hamdan, S., Rahman, M. M., and Hossen, M. F. (2015). "Impact of nanoclay on physicomechanical and thermal analysis of polyvinyl alcohol/fumed silica/clay nanocomposites," *Journal of Applied Polymer Science* 132(15), 41843. DOI: 10.1002/app.41843

Rowell, R. M. (2006) "Chemical modification of wood: A short review," *Wood Material Science and Engineering* 1(1), 29-33. DOI: 10.1080/17480270600670923

Sposito, G. (1983). "Infrared spectroscopic study of adsorbed water on reduced-charge Na/Li-montmorillonites," *Clays and Clay Minerals* 31(1), 9-16

Stolf, D. O., and Lahr, F. A. R. (2004). "Wood-polymer composite: physical and mechanical properties of some wood species impregnated with styrene and methyl methacrylate" *Journal of Materials Research* 7(4) 611-617. DOI: 10.1590/0104-1428.1868

Toh, H. K. (1979). *A Study of Diffusion in Polymers using C-14 Labelled Molecules*, Ph.D. dissertation, Loughborough University, Leicestershire, UK.

Xie, Y. J., Hill, C. A. S., Sun, D., Jalaludin, Z., Wang, Q., and Mai, C. (2011). "Effects of dynamic aging (hydrolysis and condensation) behaviour of organofunctional silanes in the aqueous solution on their penetrability into the cell walls of wood," *BioResources* 6(3), 2323-2339. DOI: 10.15376/biores.6.3.2323-2339

Xu, Y., Guo, Z., Fang, Z., Peng, M., and. Shen, L. (2013). "Combination of double-modified clay and polypropylene-graft-maleic anhydride for the simultaneously improved thermal and mechanical properties of polypropylene," *Journal of Applied Polymer Science* 128(1), 283-291. DOI: 10.1002/APP.38178

Zabel, R. A., and Morrell, J. J. (1992). *Wood Microbiology – Decay and Its Prevention*, Academic Press, San Diego, CA.

Zhao, G. J., Lv, W. H., and Xue, Z. H. (2004). "Preparation of wood/montmorillonite (MMT) intercalation nanocomposite," *Forestry Studies in China* 8(1), 35-40. DOI: 10.1007/s11632-006-0007-6

Article submitted: March 9, 2016; Peer review completed: May 28, 2016; Revised version received and accepted: June 9, 2016; Published: June 27, 2016.
DOI: 10.15376/biores.11.3.6649-6662